Available online at www.sciencedirect.com
ScienceDirect
Journal of Molecular Structure 881 (2008) 11–20
Journal of MOLECULAR STRUCTURE
www.elsevier.com/locate/molstruc

New 1,6-heptadienes with pyrimidine bases attached: Syntheses and spectroscopic analyses

Hassan H. Hammud [a,*], Amer M. Ghannoum [a], Fares A. Fares [b], Lara K. Abramian [b], Kamal H. Bouhadir [b,*]

[a] Chemistry Department, Faculty of Science, Beirut Arab University, Box 11-5020, Beirut, Lebanon
[b] Chemistry Department, Faculty of Arts & Sciences, American University of Beirut, Box 11-0236, Beirut, Lebanon

Received 19 January 2007; received in revised form 21 August 2007; accepted 22 August 2007
Available online 4 September 2007

Abstract

A simple, high yielding synthesis leading to the functionalization of some pyrimidine bases with a 1,6-heptadienyl moiety spaced from the $N-1$ position by a methylene group is described. A key step in this synthesis involves a Mitsunobu reaction by coupling ^3N-benzoyluracil and ^3N-benzoylthymine to 2-allyl-pent-4-en-1-ol followed by alkaline hydrolysis of the ^3N-benzoyl protecting groups. This protocol should eventually lend itself to the synthesis of a host of *N*-alkylated nucleoside analogs.

The absorption and emission properties of these pyrimidine derivatives (**3**–**6**) were studied in solvents of different physical properties. Computerized analysis and multiple regression techniques were applied to calculate the regression and correlation coefficients based on the equation that relates peak position λ_{max} to the solvent parameters that depend on the H-bonding ability, refractive index, and dielectric constant of solvents.

Keywords: Heptadiene; Uracil; Thymine; Mitsunobu reaction; Absorption spectra; Fluorescence

1. Introduction

Synthetic oligodeoxynucleotides (ODNs) have gained significant interest recently due to their increased role in therapeutic and diagnostic applications [1–4]. Non-conjugated heptadienes have been polymerized and copolymerized with a variety of monomers to yield polymers with interesting properties [5–7]. One approach to synthetic neutral ODNs is the polymerization of heptadienes with nucleic bases attached. Incorporation of such modified, unnatural nucleobases in oligonucleotides chain enables the application of fluorescence techniques to nucleic acid detection and to studies of conformation, dynamics and interactions of bio-molecules [8,9]. The spectroscopic study of these molecules in solution particularly their absorption and fluorescence spectra in different solvents and pH can provide useful information because most laboratory experiments as well as bio-processes occur in solution [10,11].

The ultraviolet absorption spectra of some purines and pyrimidines had been studied during the last decades [12–17]. Correlations found among the bands of pyrimidine bases and some of their derivatives show that these bands are simply derived from those of benzene [18]. Fluorescence studies of some quinolines [19,20], 2-substituted pyrimidines [21,22], 2-substituted purines [23], 5-substituted thiadiazolo and thiazolo pyrimidines [24,25] have been reported. Recently, the electronic spectra of some barbituric and thiobarbituric acids were studied in different solvents and pH, and a computerized analysis with multiple regression techniques was applied [26]. Solvent effects on the electronic absorption bands shift are commonly understood as an indication of the extent of charge reorganization of solute molecules upon electronic excitation. Conversely, solvent shifts of emission bands reflect the

* Corresponding authors. Tel.: +961 3 381862; fax: +961 1 300110.
E-mail addresses: hhammud@yahoo.com (H.H. Hammud), kb05@aub.edu.lb (K.H. Bouhadir).

0022-2860/$ - see front matter © 2007 Elsevier B.V. All rights reserved.
doi:10.1016/j.molstruc.2007.08.026

influence of equilibrium solvent arrangement around the excited solute, rearranging inertially due to the instantaneous charge redistribution upon radiative deactivation to the ground electronic state.

An effort is presented in this paper to synthesize and characterize the spectral bands of some pyrimidines derivatives and to correlate the wavelength shift (absorbance and emission) in these compounds with the variation in solvent properties and pH.

2. Equipments and reagents

Melting points were determined using a Fisher–Jones apparatus. ^{1}H NMR and ^{13}C NMR spectra were recorded in $CDCl_3$ at 300 MHz (^{1}H) or 75 MHz (^{13}C) on a Bruker AM300 NMR spectrometer. Chemical shifts are reported in parts per million (δ) downfield relative to tetramethylsilane (TMS). Multiplicities were determined by DEPT experiments. Infrared spectra were recorded as KBr pellets using a Nicolet AVATAR 360 FTIR ESP spectrometer. The IR bands are reported in wave numbers (ν, cm^{-1}). Analytical thin layer chromatography (TLC) was performed on Analtech silica gel TLC Uniplates. Column chromatography was performed with ACROS silica gel (60 Å, 200–400 mesh). Chemicals and reagents used in the various syntheses were purchased from the Aldrich Chemical Company (Milwaukee, WI) and ACROS Organics (Belgium), and were used as received. 1,4-Dioxane and tetrahydrofuran were purchased from ACROS Organics, dried over sodium metal, and then distilled directly before use.

The pH of solutions was measured on GP 353 ATC pH-meter after calibration with buffer solutions at pH's 4 and 7. The electronic absorption spectra were recorded at 25 °C on SP-3000 OPTIMA UV–Visible spectrophotometer, Japan. The room temperature spectrofluorometric measurements were carried out on a Jasco FP-6200 spectrofluorometer, Japan and supported with Jasco spectra manager software for Jasco corporation version 1.05.

The measured fluorescence intensity of the solution of compounds in different solvents was not subtracted from that of the corresponding pure solvent. The intensity scale is thus an arbitrary scale.

The electronic spectra of the solution (concentration 1×10^{-5} to 1×10^{-6} mol/l) were investigated in various organic solvents of spectroscopic grade. The solvents are of different polarities: carbon tetrachloride (CCl_4), diethyl ether, 1,4-dioxane, chloroform ($CHCl_3$), *N*,*N*-dimethylformamide (DMF), dimethyl sulfoxide (DMSO), acetonitrile (CH_3CN), ethanol (EtOH), and methanol (MeOH).

3. Synthesis of the pyrimidine derivatives

3.1. Method of preparation

3.1.1. 2-Allyl-pent-4-en-1-ol (**2**)

To a stirred suspension of lithium aluminum hydride (5.8 g, 95%, 146 mmol) in dry tetrahydrofuran (60 ml) at 0 °C (ice-water bath), a solution of acid **1** (13.6 g, 97 mmol) in dry tetrahydrofuran (75 ml) was added drop-wise and the mixture was refluxed for 21 h. The flask was then cooled to room temperature and then immersed in an ice-water bath. The reaction was quenched carefully with water (6 ml), aqueous potassium hydroxide (15%, 6 ml), and water (6 ml). The solution was filtered and the solid washed with diethyl ether. The combined filtrate and organic washes were dried over anhydrous magnesium sulphate and filtered. The solvent was evaporated under reduced pressure to yield 2-allyl-pent-4-en-1-ol (12.0 g, 98% yield). ^{1}H NMR (300 MHz) δ 1.6 (p, 1H), 2.0 (m, 4H), 2.8 (br s, 1H), 3.4 (br s, 2H), 4.9 (m, 4H), 5.7 (m, 2H); ^{13}C NMR (75 MHz) δ 35.0 (t), 40.0 (d), 64.6 (t), 116.1 (t), 136.6 (d). The spectroscopic data were in good agreement with those reported in the literature [27,28].

3.1.2. 1-(2-Allyl-pent-4-enyl)-3-benzoyl-1H-pyrimidine-2,4-dione (**3**)

To a mixture of ^{3}*N*-benzoyluracil (4.32 g, 20 mmol), 2-allyl-pent-4-en-1-ol (3.02 g, 24 mmol), and triphenyl phosphine (6.3 g, 24 mmol) in dry dioxane (130 ml) at 0 °C was added drop-wise a solution of diisopropyl azodicarboxylate (DIAD, 94%, 5.16 g, 24 mmol) in dry dioxane (30 ml) under a nitrogen atmosphere over 30 min. The mixture was stirred at room temperature overnight to yield a clear solution. The solvent was evaporated under reduced pressure to give an oily residue from which some triphenylphosphine oxide and diisopropyl hydrazodicarboxylate crystallized overnight. The solid was filtered and washed with a small amount of diethyl ether. The filtrates were combined and concentrated under reduced pressure and the residue was purified by column chromatography using dichloromethane:acetone (9:1) to yield the 1-(2-allyl-pent-4-enyl)-3-benzoyl-1H-pyrimidine-2,4-dione as a white solid (4.47 g, 69% yield). M.p. 74–75 °C; ^{1}H NMR (300 MHz) δ 2.1 (m, 5H), 3.66 (d, $J = 3.9$ Hz, 2H), 5.09 (m, 4H), 5.75 (m, 2H), 5.79 (d, $J = 7.95$ Hz, 1H), 7.21 (d, $J = 7.98$ Hz, 1H), 7.52 (m, 2H), 7.64 (m, 1H), 7.92 (m, 2H); ^{13}C NMR (75 MHz) δ 35.6 (t), 36.8 (d), 52.8 (t), 101.8 (d), 117.7 (t), 129.2 (d), 130.4 (d), 131.4 (s), 135.1 (d), 144.8 (d), 149.9 (s), 162.4 (s), 168.7 (s); FTIR (KBr disk, cm^{-1}) 3099, 3072, 2974, 2928, 1749, 1697, 1652, 1624, 1595, 1446, 1384, 1338, 1350, 1255, 1105, 978, 918, 804, 783, 763, 700, 680, 630; HRMS (EI) calcd for $C_{19}H_{20}N_2O_3$ (M^+), 324.14739, found 324.14751.

3.1.3. 1-(2-Allyl-pent-4-enyl)-1H-pyrimidine-2,4-dione (**4**)

To a solution of sodium metal (0.75 g, 32.6 mmol) in methanol (35 ml) at 0 °C (ice-water bath) under a nitrogen atmosphere was added drop-wise a solution of **3** (1.08 g, 3.33 mmol) in methanol (20 ml) and the mixture was refluxed for 4 h then stirred at room temperature overnight. The solvent was evaporated under reduced pressure and the residue was dissolved in dichloromethane (20 ml) and washed with aqueous hydrochloric acid (10%, 10 ml) and then with aqueous saturated solution of sodium bicarbonate (10 ml). The organic layer was dried over anhy-

drous magnesium sulphate, filtered, and the solvent was removed under reduced pressure to yield a white solid that was purified by flash chromatography using dichloromethane: acetone (9:1) to afford **4** as a white solid (623 mg, 85% yield). M.p. 87–88 °C; ^{1}H NMR (300 MHz) δ 2.10 (m, 5H), 3.65 (d, 2H, $J = 6.03$ Hz), 5.10 (m, 4H), 5.73 (d, $J = 7.86$ Hz, 1H), 5.79 (m, 2H), 7.13 (d, $J = 7.86$ Hz, 1H), 10.0 (br. s, NH); ^{13}C NMR (75 MHz) δ 35.4 (t), 36.9 (d), 52.2 (t), 101.9 (d), 117.5 (t), 135.1 (d), 145.0 (d), 151.3 (s), 164.2 (s); FTIR (KBr disk, cm^{-1}) 3016.5, 2978, 2916, 1701, 1670, 1464, 1406, 1387, 1360, 1340, 1279, 1248, 1232, 1178, 993, 916, 767, 551; HRMS (EI) calcd for $C_{12}H_{16}N_2O_2$ (M^+), 220.12118, found 220.11989.

3.1.4. 1-(2-Allyl-pent-4-enyl)-3-benzoyl-5-methyl-1H-pyrimidine-2,4-dione (5)

To a mixture of ^{3}*N*-benzoylthymine (4.6 g, 20 mmol), 2-allyl-pent-4-en-1-ol (3.02 g, 24 mmol), and triphenyl phosphine (6.3 g, 24 mmol) in dry dioxane (130 ml) at 0 °C was added drop-wise a solution of diisopropyl azodicarboxylate (DIAD, 94%, 5.16 g, 24 mmol) in dry dioxane (30 ml) under a nitrogen atmosphere over 30 minutes. The mixture was stirred at room temperature overnight to yield a clear solution. The solvent was evaporated under reduced pressure to give an oily residue from which some triphenylphosphine oxide and diisopropyl hydrazodicarboxylate crystallized overnight. The solid was filtered and washed with a small amount of diethyl ether. The filtrates were combined and concentrated under reduced pressure and the residue was purified by column chromatography using dichloromethane:acetone (9:1) to afford 1-(2-allyl-pent-4-enyl)-3-benzoyl-5-methyl-1H-pyrimidine-2,4-dione as a white solid (5.2 g, 77% yield). M.p. 84–85 °C; ^{1}H NMR (300 MHz) δ 1.93 (s, 3H), 2.1 (m, 5H), 3.63 (d, $J = 4.6$ Hz, 2H), 5.09 (m, 4H), 5.78 (m, 2H), 7.08 (s, 1H), 7.47 (m, 2H), 7.64 (m, 1H), 7.89 (m, 2H); ^{13}C NMR (75 MHz) δ 12.1 (q), 35.2 (t), 36.8 (d), 52.1 (t), 109.8 (d), 117.3 (t), 129.2 (d), 130.2 (d), 131.5 (s), 135.4 (d), 141.4 (s), 149.9 (s), 163.1 (s), 169.3 (s); FTIR (KBr disk, cm^{-1}) 3072, 2974, 2927, 1745, 1697, 1647, 1599, 1442, 1345, 1321, 1225, 1115, 980, 956, 908, 875, 789, 762, 675; HRMS (EI) calcd for $C_{20}H_{22}N_2O_3$ (M^+), 338.16304, found 338.16295.

3.1.5. 1-(2-Allyl-pent-4-enyl)-5-methyl-1H-pyrimidine-2,4-dione (6)

To a solution of sodium metal (1.88 g, 81.5 mmol) in methanol (85 ml) at 0 °C (ice-water bath) under a nitrogen atmosphere was added drop-wise a solution of 5 (2.82 g, 8.33 mmol) in methanol (50 ml) and the mixture was refluxed for 4 h then stirred at room temperature overnight. The solvent was evaporated under reduced pressure and the residue was taken up in dichloromethane (40 ml) and washed with aqueous hydrochloric acid (10%, 20 ml) and then with saturated solution of sodium bicarbonate (20 ml). The organic layer was dried over anhydrous magnesium sulphate. Removal of the solvent under reduced pressure gave a white solid that was purified by flash chromatography using dichlromethane:acetone (9:1) to yield **6** as a white solid (1.52 g, 78% yield). M.p. 111–113 °C; ^{1}H NMR (300 MHz) δ 1.92 (s, 3H), 2.09 (m, 5H), 3.63 (d, $J = 6.12$ Hz, 2H), 5.08 (m, 4H), 5.75 (m, 2H), 6.98 (s, 1H), 10.3 (br. s, NH); ^{13}C NMR (75 MHz) δ 12.3 (q), 35.4 (t), 37.1 (d), 51.8 (t), 110.4 (d), 117.2 (t), 135.5 (d), 141.0 (s), 151.6 (s), 164.9 (s); FTIR (KBr disk, cm^{-1}) 3161, 3022, 2982, 2835, 1660, 1477, 1456, 1427, 1379, 1367, 1348, 1313, 1279, 1246, 1115, 993, 945, 914, 889, 862, 764, 563; HRMS (EI) calcd for $C_{13}H_{18}N_2O_2$ (M^+), 234.13683, found 234.13649.

3.2. Results and discussion

We report herein, the synthesis of 1,6-heptadienes with uracil and thymine connected to carbon-4 of the former via a methylene spacer. The synthetic protocol was initiated with the 2-allyl-pent-4-enoic acid **1** that was prepared in our laboratory following a reported procedure [29]. Reduction of compound **1** to the corresponding primary alcohol, 2-allyl-pent-4-en-1-ol **2**, was achieved with lithium aluminum hydride (LAH) in 98% yield [27,28] (Scheme 1). The ^{3}*N*-protected uracil and thymine bases have been prepared following reported procedures [30]. The Mitsunobu reaction was then employed to couple the ^{3}*N*-protected nucleic bases to 2-allyl-pent-4-en-1-ol **2** utilizing triphenylphosphine and diisopropyl azodicarboxylate (DIAD) in dry dioxane to yield the heptadiene derivatives **3** and **5** in 69% and 77% yield, respectively [31–34].

Examination of the ^{1}H NMR spectra of **3** and **5** revealed the aromatic protons of the benzoyl group resonating in the δ 7.5–8.0 ppm region. Further evidence for the formation of **3** and **5** was clearly indicated in the ^{13}C NMR spectra by the absence of the carbon resonating at δ 65.1 ppm (carbon singly connected to an oxygen) and the presence of a less deshielded carbon resonating at δ 52.8 ppm and δ 52.1 ppm in the spectrum of **3** and **5**, respectively, indicating carbons singly connected to the less electronegative nitrogen.

The ^{3}*N*-benzoyl groups of intermediates **3** and **5** were then hydrolyzed in a methanolic solution of sodium methoxide to yield the target compounds 1-(2-allyl-pent-4-enyl)-1H-pyrimidine-2,4-dione **4** and 1-(2-allyl-pent-4-enyl)-5-methyl-1H-pyrimidine-2,4-dione **6** in 85% and 78% yield, respectively (Scheme 1). The formation of **4** and **6** was clearly elucidated in the ^{1}H NMR spectra by the two broad singlets at 10.0 ppm (for **4**) and 10.2 ppm (for **6**) due to the NH protons in the heterocyclic ring. This was confirmed further by the absence of signals for the aromatic protons resonating in the δ 7.5–8.0 ppm region in the ^{1}H NMR spectra of both **4** and **6**.

4. UV absorption and fluorescence study of the pyrimidine derivatives (3–6)

4.1. Method of calculations

The solvent effect and that of the specific interaction between solute and solvent molecules (hydrogen bonding)

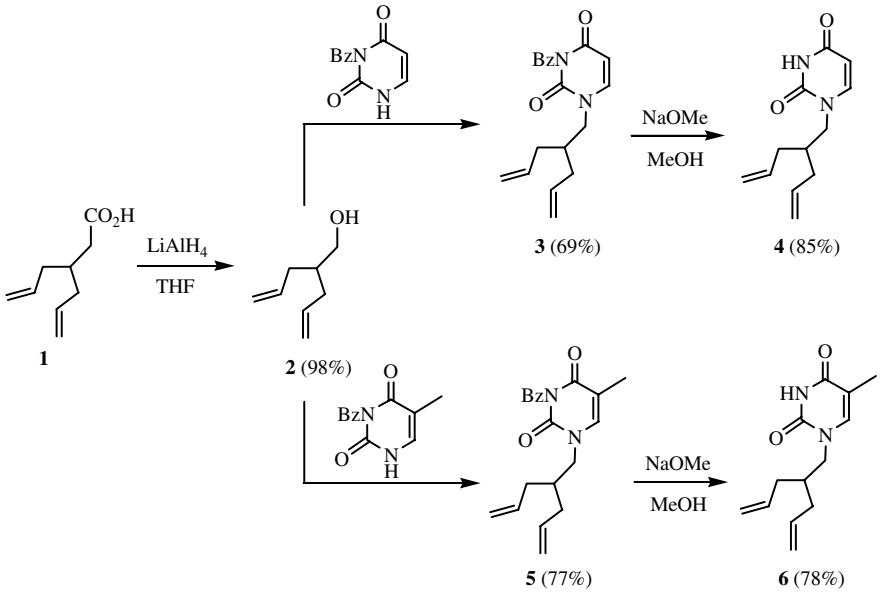

Scheme 1.

are major factors to explain the spectral behaviour of compounds. In the regression analysis, the following equation is used:

$$Y = a_0 + a_1X_1 + a_2X_2 + a_3X_3 + \cdots$$

The constant a_1, a_2, and a_3 are the different regression coefficients, and the constant a_0 is the regression intercept. The observed peak location λ_{max} (Y) is considered as the dependent variable while the independent variables have been selected to be the solvent interaction mechanisms (D, n, E) and (E, K, M, N) (Table 1).

The parameter E is an empirical solvent polarity parameter sensitive to both solvent–solute hydrogen bonding and dipolar interactions. K depends on the solvent dielectric constant D, and is a measure of the polarity of the solvent, $K = (D - 1)/(2D+1)$.

M depends on the solvent refractive index n and is a measure of solute permanent dipole–solvent induced dipole interactions, $M = (n^2 - 1)/(2n^2 + 1)$. N is a measure of permanent dipole–permanent dipole interactions, $N = (D - 1)/(D + 2) - (n^2 - 1)/(n^2 + 2)$. A multiple regression analysis has been performed; in each case fits are obtained as a function of one parameter, two parameters or three parameters. The results are listed in Tables 4–11.

In a complementary study the coefficients K_1, K_2, v vapour were calculated using multiple regression technique based on the following equation:

$$v_{solution} = v_{vapour} + K_1(2D - 2)/(2D + 1) + K_2(2n^2 - 2)/(2n^2 + 1)$$

v_{vapour} is the frequency of the maximum in absence of solvents. D is the dielectric constant, and n is the refractive index of the solvents. As an indication of the goodness of the fit, the multiple correlation coefficient and the square of correlation were calculated for each $r^2(v, n^2)$, and $r^2(v, D)$; the results are summarized in Table 12. The emission spectra were recorded in different solvents, and the Stokes shift is correlated with the orientation polarizability Δf (function of dielectric constant D and refractive index n) of the solvents.

4.2. Results and discussion

The electronic absorption (Table 2 and Figs. 1, 2) and fluorescence emission (Table 3 and Figs. 4–6) spectra for each compound were recorded in a variety of solvents of

Table 1
Solvent dielectric constant D, refractive index n, empirical polarity E, and parameters used in spectral correlation equations

Solvent	D	n	E	K	M	N
CCl_4	2	1.426	32.5	0.2	0.22	0.01
Diethyl ether	4.2	1.353	34.6	0.34	0.18	0.3
1,4-Dioxane	2.2	1.422	36	0.22	0.2	0.03
Chloroform	4.7	1.443	39.1	0.36	0.21	0.29
Water	78.5	1.33	63.1	0.49	0.17	0.76
Dimethylformamide	36.7	1.427	43.8	0.48	0.2	0.67
Dimethyl sulfoxide	48.9	1.478	45	0.49	0.22	0.66
Acetonitrile	37.5	1.344	46	0.48	0.18	0.71
Ethanol	24.3	1.361	51.9	0.47	0.18	0.67
Methanol	32.6	1.329	55.5	0.48	0.17	0.71

Table 2
λ_{max}(abs) of compounds (**3**–**6**) in solvents of different polarities

Solvents	Compound **3**	Compound **4**	Compound **5**	Compound **6**
CCl_4	261, 277	268	262, 283	274
Ether	252, 280	265	250, 282	270
Dioxane	255, 279	267	255, 283	272
Chloroform	256, 280	269	256, 284	275
DMF	270	272	271	275
DMSO	264	270	264	275
Acetonitrile	255, 278	268	254, 280	273
Ethanol	255, 280	269	254, 283	274
Methanol	255, 280	269	255, 283	274

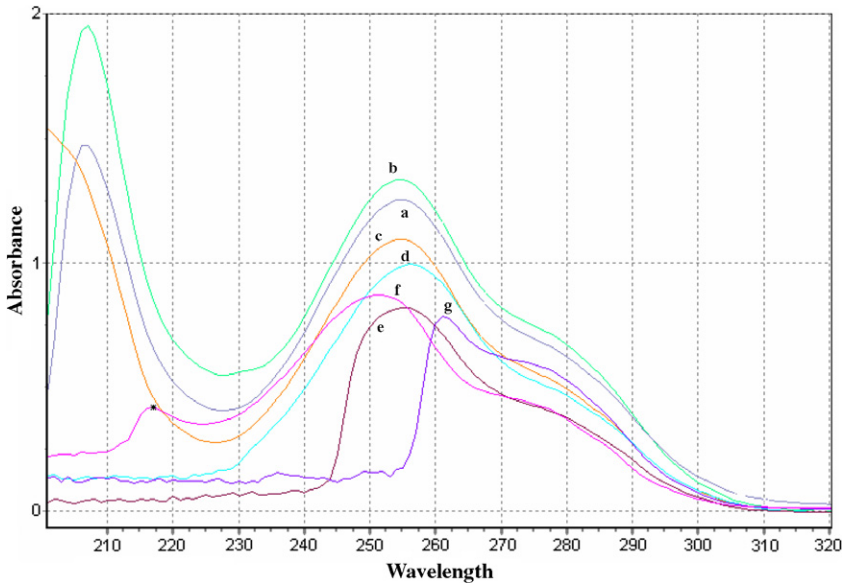

Fig. 1. Electronic absorption spectra of **3** in different solvents: (a) methanol, (b) ethanol, (c) acetonitrile, (d) chloroform, (e) 1,4-dioxane, (f) diethyl ether, and (g) carbon tetrachloride.

different physical properties, mainly the dielectric constant (ε) and the refractive index (n). Generally, the effect of solvents on the absorption bands of these substances consists of displacements and does not involve a fundamental change of the general form of the spectrum [35–38]. The absorption and emission spectra of these compounds are perturbed by varying the organic solvents, and the spectral shifts are different for the absorption spectrum from those for the emission one.

4.2.1. Spectrophotometric study

4.2.1.1. Absorption electronic spectra. The electronic absorption spectra of compounds **4** and **6** show strong absorption band (Band A) in the range 265–275 nm due to π–π^* electronic transitions and exhibit red shift (compound **4**, Table 2) as proceeding from non-polar (CCl_4, $\lambda_{max} = 268$ nm) to polar solvents (DMF, $\lambda_{max} = 272$ nm) due to the stabilization of π^* orbital more than π orbital. Also, the first band (Band A) in the range 250–272 nm (compounds **3** and **5**) exhibit π–π^* electronic transitions with high molar absorptivities and bathochromic shift while proceeding from CCl_4 ($\lambda_{max} = 261$ nm) and diethyl ether ($\lambda_{max} = 252$ nm) to the more polar solvents DMF ($\lambda_{max} = 270$ nm) and DMSO ($\lambda_{max} = 264$ nm) (compound **3**, Table 2) that substantiate their π–π^* nature. The band (Band B) at about 280 nm (compounds **3** and **5**) is associated with considerable intramolecular charge transfer character [39,40] whose nature is substantiated by its broadness

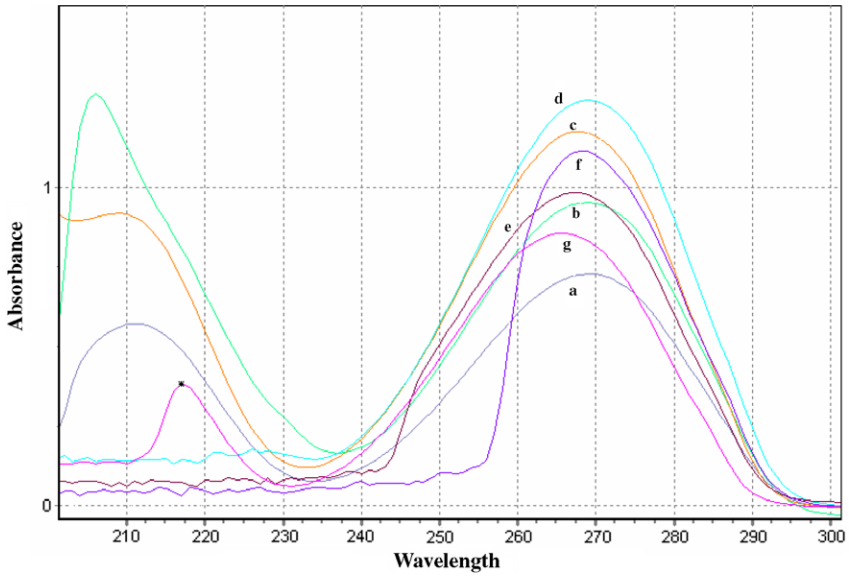

Fig. 2. Electronic absorption spectra of **4** in different solvents: (a) methanol, (b) ethanol, (c) acetonitrile, (d) chloroform, (e) 1,4-dioxane, (f) carbon tetrachloride, and (g) diethyl ether.

Table 3
λ_{abs}, λ_{em}, Δv(cm^{-1}) for compounds (**3**–**6**) and Δf values in different solvents

Solvent	Compound	λ_{abs}	λ_{em}	Δv	Δf
Diethyl ether	**3**	252	343	10528	0.162
	4	265	305	4948.96	
	5	250	345	11014.5	
	6	270	311	4882.7	
Dioxane	**3**	255	311	7061.3	0.02
	4	267	303	4449.8	
	5	255	313	7266.8	
	6	272	307	4191.4	
$CHCl_3$	**3**	256	359	11207.3	0.148
	4	269	335	7323.9	
	5	256	360	11284.7	
	6	275	336	6601.7	
DMF	**3**	270	328	6549.2	0.274
	4	272	329	6369.5	
	5	271	329	6505.2	
	6	275	332	6243.15	
DMSO	**3**	264	326	7203.9	0.263
	4	270	330	6734.0	
	5	264	326	7203.9	
	6	275	335	6512.3	
CH_3CN	**3**	255	313	7266.8	0.305
	4	268			
	5	254	313	7421.2	
	6	273			
Ethanol	**3**	255	323	8255.9	0.289
	4	269	326	6499.8	
	5	254	322	8314.1	
	6	274	330	6193.3	
Methanol	**3**	255			0.309
	4	269			
	5	255	332	9095.2	
	6	274	339	6997.8	

Table 4
Regression analysis for compound **3** at $\lambda_{abs} = 255$ nm using *D*, *n*, and *E* solvent parameters

Parameters	a_0	a_1	a_2	a_3	MCC
D	254.984	0.146			0.466
n	161.461	69.129			0.626
E	258.424	−0.007			0.01
D, *n*	154.453	0.148	69.725		0.784
D, *E*	273.798	0.305	−0.521		0.679
n, *E*	129.288	0.239	36.261		0.691
D, *n*, *E*	180.192	−0.18	58.108	0.203	0.796

and its sensitivity to the nature of solvent used and is confirmed by its spectral behaviour in buffer solution of different pH values.

The absence of the n–π^* in the spectra of these compounds can be presumably ascribed to its submerging with a strong (280 nm) intramolecular charge transfer band (**3**, **5**) and of the π–π^* band (**4**, **6**).

4.2.1.2. Solvatochromism absorption correlation studies. From the correlation of λ_{max} (Band A) for compounds **3**–**6** with any of solvent parameters, an idea about the type of interactions between the solute and solvent can be obtained. The solvatochromic shift reveals the effect of dielectric constant and refractive index of solvent as well as H-bond interaction.

A one parameter correlation between λ_{max} of compounds **3**–**6** with either *D*, *n*, or *E* parameters reveal a high dependence of λ_{max} (compounds **3** and **5**) on the refractive index with MCC > 0.6 compared to that of **4** and **6** with MCC < 0.5. The correlation for *E* parameter with λ_{max} in case of compound **3** and **5** indicate no remarkable solute–solvent hydrogen bond interaction (MCC < 0.03) compared to that of **4** and **6** with MCC > 0.4 indicating solute–solvent hydrogen bonding interactions present along with dipole interactions.

Correlation with two parameters equation for hydrogen bonding and refractive index (MCC > 0.8) prove higher influence of these two parameters on the position of λ_{max} for compounds **4** and **6** than that of the dielectric constant and hydrogen bonding (MCC = 0.645) or dielectric constant and refractive index (MCC = 0.763) (Tables 5–7).

The correlations for compounds **3** and **5** show no remarkable solute–solvent hydrogen bonding interactions compared to compounds **4** and **6** due to the presence of the benzoyl group at the N(3) position that substituted the amino (NH) hydrogen atom, but a (*D*, *n*) interaction with correlation of (MCC = 0.784 and 0.763) for **3** and **5**, respectively (Tables 4–6). Little improvement of fits was shown when using three parameters *D*, *n*, and *E* in case of compounds (**4**–**6**) indicating their influence in different manner.

The correlations between λ_{max} of compounds (**3**–**6**) with either *E* (solvent polarity parameter), *K* (function of dielectric constant), *M* (function of refractive index), or *N* (measure of permanent dipole–permanent dipole interaction) parameters (Tables 8–11) show dependence of λ_{max} of compound **3** on *M* parameter (MCC > 0.5), and that of compound **5** on *K* parameter (MCC > 0.5), but relatively similar dependence of λ_{max} of compounds **4** and **6** on each parameter.

Higher correlation is shown in compound **3** using two parameters equation (Table 8) with either (*KM*, MCC = 0.759) or (*MN*, MCC = 0.785) than with (*EM*, MCC = 0.686), (*EN*, MCC = 0.436) or (*KN*, MCC = 0.238) parameters.

Compound **5** show higher correlation (Table 10) between λ_{max} and *KM*, *KN* or *EK*, with a MCC > 0.7 showing a more influence of the polarity parameter on the spectra than in case of compound **3**.

Compounds **4** and **6** show high correlation (Tables 9 and 11) between the parameter *K* and the *N* parameter (MCC > 0.79) or the *E* parameter (MCC > 0.8); improvement of fits when using three parameters *E*, *K*, and *M* or *N* since higher correlation coefficients (MCC > 0.8) are obtained.

The values of K_1, K_2, v (vapour), r^2 (v, *D*), r^2 (v, *n*) and MCC for solutes are computed and listed in Table 12. The data indicated that both the dielectric constant and the refractive index of solvents affect the electronic absorption spectra of compounds but with varying degree.

Table 5
Regression analysis for compound **4** at $\lambda_{abs} = 269$ nm using *D*, *n*, and *E* solvent parameters

Parameters	a_0	a_1	a_2	a_3	MCC
D	267.094	0.068			0.644
n	247.584	15			0.402
E	263.505	0.118			0.478
D, *n*	245.726	0.069	15.276		0.763
D, *E*	266.812	0.066	0.008		0.645
n, *E*	220.628	28.173	0.2		0.83
D, *n*, *E*	225.836	25.437	0.157	0.021	0.839

Table 6
Regression analysis for compound **5** at $\lambda_{abs} = 254$ nm using *D*, *n*, and *E* solvent parameters

Parameters	a_0	a_1	a_2	a_3	MCC
D	254.671	0.15			0.424
n	145.888	80.109			0.641
E	258.667	−0.18			0.022
D, *n*	141.756	0.153	80.723		0.772
D, *E*	274.828	0.321	−0.558		0.632
n, *E*	110.229	0.264	97.535		0.702
D, *n*, *E*	158.901	0.194	71.964	−0.135	0.778

Table 7
Regression analysis for compound **6** at $\lambda_{abs} = 274$ nm using *D*, *n*, and *E* solvent parameters

Parameters	a_0	a_1	a_2	a_3	MCC
D	272.624	0.043			0.479
n	251.618	15.691			0.49
E	269.89	0.086			0.404
D, *n*	250.427	0.044	15.868		0.689
D, *E*	271.668	0.035	0.026		0.487
n, *E*	229.733	0.162	26.386		0.845
D, *n*, *E*	226.019	0.193	28.337	−0.015	0.851

4.2.1.3. pH effect on absorption spectra. The effect of pH change on the electronic absorption spectra of solutions of each of the compounds (**3**, **4**, **5**, and **6**) was studied in ethanol by adding 1 ml of universal buffer in the pH range 3.2–12 and the extreme pH (1.4 and 13.2) were obtained by adding few drops of aqueous HCl (0.1 N) or aqueous NaOH (0.1 N), respectively. The absorption spectra of these compounds in different buffers show little shift in λ_{max}(abs), (Table 13, Fig. 3).

All four compounds show red shift in λ_{max}(abs) as proceeding from ethanolic solution to pH = 1.4; this red shift is due to the protonation of non-bonded pair on carbonyl group causing stabilization of the excited state relative to the ground state (protonation at an amino group cause a blue shift upon protonation) [41,42].

Compounds **3** and **5** show further red shift as proceeding to basic solutions indicating a greater degree of interaction between the substituents and the aromatic ring [13]. The blue shift in the absorption spectra of compounds **4** and **6** in basic solutions could be due to the formation of different tautomeric forms [43] also could be related to acid base equilibrium.

Table 8
Regression analysis coefficients for compound **3** at $\lambda_{abs} = 255$ nm using *E*, *K*, *M*, and *N*

	a_0	a_1	a_2	a_3	MCC
E	258.424	−0.07			0.01
K	253.813	10.99			0.223
M	223.85	175.197			0.572
N	256.27	4.091			0.209
EK	263.51	−0.466	37.041		0.417
EM	194.015	0.336	254.405		0.686
EN	274.404	−0.561	17.045		0.436
KM	199.933	26.967	243.569		0.759
KN	247.773	39.619	−11.461		0.238
MN	201.587	261.754	11.858		0.785
EKM	202.223	−0.05	29.397	237.928	0.76
EKN	277.453	−0.579	−11.564	21.991	0.437
EMN	210.733	−0.182	246.124	15.595	0.793
KMN	213.253	−92.198	300.289	49.201	0.819

Table 9
Regression analysis coefficients for compound **4** at $\lambda_{max} = 269$ nm using *E*, *K*, *M*, and *N*

	a_0	a_1	a_2	a_3	MCC
E	263.505	0.118			0.478
K	262.858	29.134			0.282
M	264.919	9.299			0.559
N	266.941	3.587			0.544
EK	242.333	0.231	83.626		0.821
EM	264.701	0.01	8.716		0.559
EN	266.718	0.007	3.427		0.544
KM	250.932	63.227	13.447		0.79
KN	252.191	70.609	5.682		0.813
MN	263.2	17.466	−3.261		0.563
EKM	244.047	0.15	80.185	6.14	0.845
EKN	245.488	0.133	82.063	2.944	0.85
EMN	261.215	0.039	20.869	−5.498	0.568
KMN	254.289	77.589	−16.582	12.398	0.822

Table 10
Regression analysis coefficients for compound **5** at $\lambda_{abs} = 254$ nm using *E*, *K*, *M*, and *N*

	a_0	a_1	a_2	a_3	MCC
E	258.667	−0.18			0.022
K	217.315	207.48			0.599
M	254.192	9.452			0.17
N	256.307	3.515			0.159
EK	183.226	0.384	297.98		0.71
EM	263.339	−0.439	34.026		0.339
EN	273.43	−0.53	15.746		0.357
KM	192.781	177.615	27.662		0.751
KN	194.137	297.595	12.346		0.771
MN	248.898	34.547	−10.046		0.181
EKM	190.179	0.057	284.024	24.901	0.752
EKN	198.272	−0.82	290.528	14.035	0.778
EMN	277.181	−0.551	−14.227	21.831	0.359
KMN	209.028	347.141	−117.695	60.016	0.821

4.2.2. Fluorescence study

4.2.2.1. Fluorescence measurements. Compounds (**3**–**6**) fluoresce at room temperature [44–46]. The excitation wavelength was fixed at 254 nm for compounds (**3** and **5**),

Table 11
Regression analysis coefficients for compound **6** at $\lambda_{abs} = 274$ nm using *E*, *K*, *M*, and *N*

	a_0	a_1	a_2	a_3	MCC
E	269.89	0.086			0.404
K	265.78	39.764			0.448
M	271.353	5.633			0.395
N	272.616	2.089			0.369
EK	247.611	0.205	87.999		0.913
EM	270.26	0.052	2.698		0.418
EN	270.292	0.072	0.429		0.406
KM	257.013	64.826	9.885		0.775
KN	257.946	70.219	4.172		0.792
MN	268.041	21.328	−6.284		0.424
EKM	247.574	0.206	88.073	−0.132	0.913
EKN	247.514	0.208	88.047	−0.9	0.913
EMN	261.855	0.121	31.997	−13.256	0.5
KMN	259.415	75.107	−11.611	8.875	0.798

while that of (**4** and **6**) at 269 nm. The shape of the excitation spectrum is shown to coincide reasonably well with the absorption spectrum. The fluorescence excitation spectra were measured on samples with maximum absorbance less than 0.1 in order to avoid inner filter distortion.

The emission wavelength (λ_{max}) measured in different solvents are shown in Table 3. Compound **3** show a hypsochromic shift (Fig. 4) in λ_{em} while proceeding from diethyl ether (343 nm) to DMF (328 nm) and DMSO (326 nm) that validates an n–π^* transition. The same was noticed in case of compound **5** where emissions at 360 nm in chloroform and 345 nm in diethyl ether show a blue shift (Table 3) to 326 nm in DMSO and 329 nm in DMF. Compounds (**3** and **5**) show no fluorescence in CCl_4 due most probably to that this non-polar solvent cannot form a hydrogen-bonded complex with the solutes [25].

Compounds **4** and **6** show a red shift in emission spectra (Figs. 5 and 6) as proceeding from diethyl ether (305 and 311 nm, respectively) to DMF (329 and 332 nm, respectively) and DMSO (330 and 335 nm, respectively), due to π–π^* transition [22]. Fluorescence quenching in acetonitrile (compounds **4** and **6**) is observed due to lone pair donor–acceptor interaction. No fluorescence was observed in CCl_4 (compound **4** and **6**) because the lowest excited singlet state is of the n–π^* type and favours radiationless intersystem crossing as a mode of deactivation of the lowest excited singlet state. The addition of small amounts of acid results in hydrogen bonding with the non-bonded pairs raising the energy of the n–π^* state to such a degree that the lowest π–π^* state becomes the lowest excited singlet state making fluorescence to occur [25].

4.2.2.2. Solvent effect on the fluorescence properties. The fluorescence emission spectra showed considerable spectral shifts in the organic solvents (Table 3, Figs. 4–6). The spectral shift is correlated with the polarity parameters (dielectric constant and refractive index) of the solvents. Stokes shift ($\nu_a - \nu_{em}$), is one of the quantitative parameters which is useful to understand the origin of the variation of spectral shift in organic solvents.

The large Stokes shift (Table 3) indicated an increase in the dipole moment upon excitation. This behaviour has been attributed to a charge redistribution of the excited state with respect to the ground state.

The plots of ($\nu_a - \nu_{em}$) versus the solvent polarity parameter Δf for the compounds (**3**–**6**) in solvents of different polarities ($\Delta f = [(D-1)/(2D+1) - (n^2-1)/(2n^2+1)]$) show the presence of linear correlation of Stokes shift with Δf in polar and non-polar solvents ($r^2 > 0.85$) for compounds (**4** and **6**) with a slight deviation in chloroform ($r^2 = 0.65$), but only a satisfactory linear relationship in the aprotic ($r^2 > 0.9$) solvents for compounds (**3** and **5**). The plots show linear correlation that is in good agreement with Lippert–Mataga equation [47–49] and confirms that the slope depends upon the change in dipole moment upon excitation.

$$(\nu_a - \nu_{em}) = \frac{2(\mu_e - \mu_g)^2}{hca^3} \times \left(\frac{(D-1)}{(2D+1)} - \frac{(n^2-1)}{(2n^2+1)}\right) + K$$

"ν_a" and "ν_{em}" are the peak absorption and emission frequencies per centimeter, "μ_e" and "μ_g" are the dipole moment of each compound in excited and ground state, "*D*" and "*n*", are the dielectric constant and refractive index of the solvent, respectively, "*h*" is the Planck's constant, "*c*" is the speed of light and "*a*" the Onsager cavity radius for each molecule, "*K*" is a constant.

4.2.2.3. pH effect. The emission spectra of these compounds show little dependence of the position of λ_{max} (emission) on the pH of solution, but show slight enhancement of the fluorescence intensity at low pH due to the formation of cationic species, and of quenching at pH greater than 7 due to the formation of anionic species with non-fluorescing properties.

5. Conclusion

In summary, we have synthesized two examples of non-conjugated dienes with uracil and thymine attached and separated from carbon-4 of the former by a methylene spacer. This protocol constitutes a simple,

Table 12
K_1, K_2, ν(vapour), and correlation analysis data for the compounds (**3**–**6**) at different ν (cm^{-1})

Compound	ν(vap) (cm^{-1})	K_1	K_2	MCC	$r^2(\nu, D)$	$r^2(\nu, n)$
3	46688.35	−1531.03	−17373.4	0.749	0.217	0.4
4	40436.85	−1954.5	−3901.37	0.7	0.343	0.002
5	47636.95	−1511.64	−19761.2	0.737	0.179	0.421
6	38492.19	−539.356	−3907.39	0.72	0.229	0.238

Table 13
λ_{max}(abs) of compounds (**3**–**6**) in different pH

pH	ETOH	pH 1.4	pH 3.2	pH 5.1	pH 7.4	pH 9.7	pH 12.5	pH 13.2
Compound **3**	255	256	256	256	256	257	257	260
Compound **4**	269	270	270	270	270	269	268	267
Compound **5**	254	256	256	256	256	257	257	258
Compound **6**	274	275	275	275	275	274	273	273

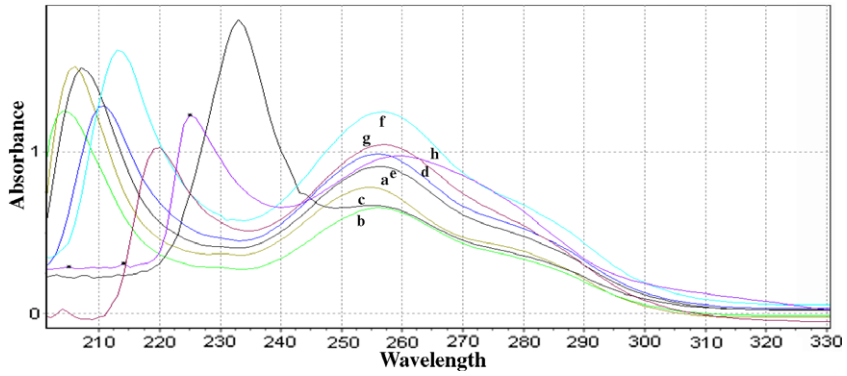

Fig. 3. Electronic absorption spectra of **3** in different pH: (a) ethanol, (b) pH 1.4, (c) pH 3.2, (d) pH 5.1, (e) pH 7.4, (f) pH 9.7, (g) pH 12.5, and (h) pH 13.2.

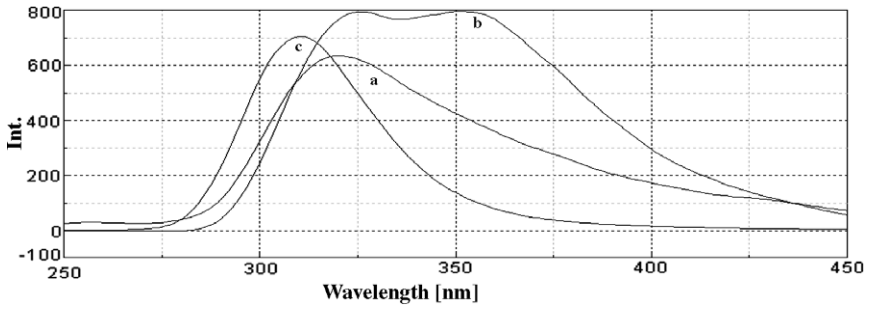

Fig. 4. Fluorescence spectra of solutions of compound **3** at $\lambda_{ex} = 254$ nm in different solvents: (a) ethanol, (b) dimethyl sulfoxide, and (c) 1,4-dioxane.

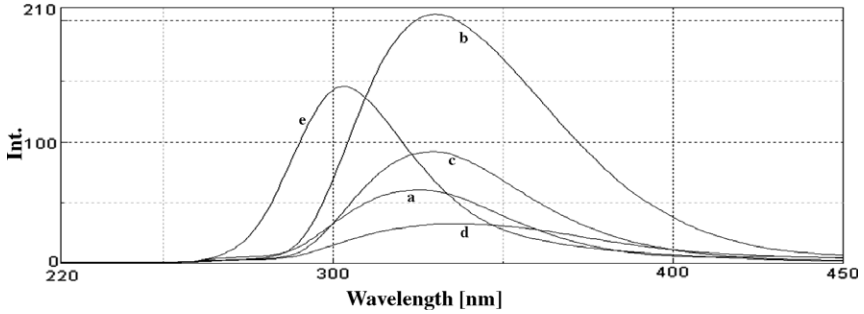

Fig. 5. Fluorescence spectra of solutions of compound **4** at $\lambda_{ex} = 269$ nm in different solvents: (a) ethanol, (b) dimethyl sulfoxide, (c) dimethylformamide, (d) chloroform, and (e) 1,4-dioxane.

high yielding procedure that could be applied for the synthesis of similar derivatives with other nucleic bases and heterocycles as well. These molecules are attractive precursors for the synthesis of neutral carbocyclic nucleoside and polynucleotide analogs. The absorption and fluorescence spectra of these compounds show significant dependence on specific and non-specific solute–solvent interactions.

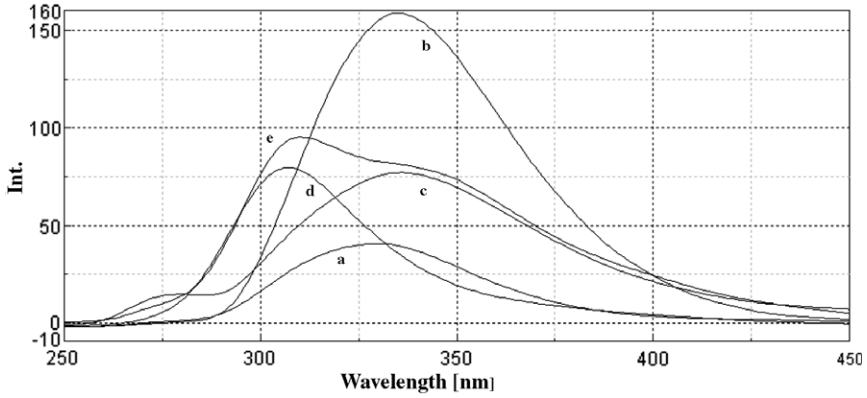

Fig. 6. Fluorescence spectra of solutions of compound **6** at $\lambda_{ex} = 269$ nm in different solvents: (a) ethanol, (b) dimethyl sulfoxide, (c) chloroform, (d) 1,4-dioxane, and (e) diethyl ether.

Acknowledgements

The authors are grateful to the University Research Board (URB) at the American University of Beirut and the Lebanese National Council for Scientific Research (LNCSR) for financial support.

References

[1] E. Uhlmann, A. Peyman, Chem. Rev. 90 (1990) 543.
[2] S. Agrawalides, Biochem. Biophys. Acta 1489 (1999) 53.
[3] M. Han, J. Polynucleotide Analogues. Adv. Polym. Sci. 153 (2000) 1.
[4] K. Miller, K. Sudip, Pharm. Sci. Technol. Today 1 (1998) 377.
[5] G. Butler, Cyclopolymerization and Cyclocopolymerization, Marcel Dekker Inc., New York, NY, 1992 (Chapter 2).
[6] J. Tsai, P. Shevlin, J. Org. Chem. 63 (1998) 3230.
[7] J. Tsai, K. Bouhadir, J. Zhou, T. Webb, Y. Sun, P. Shevlin, J. Org. Chem. 68 (2003) 1235.
[8] A. Mayer, S. Neuenhofer, Angew. Chem Int. Ed. Engl. 33 (1994) 1044.
[9] M. O'Donnell, L. McLaughlin, in: S.M. Hecht (Ed.), Bioorganic Chemistry: Nucleic Acids, Oxford University Press, NY, 1996, pp. 216–243.
[10] C. Cramer, D. Truhlar, Chem. Rev. 99 (1999) 2161.
[11] C. Reichardt, Solvents and Solvent effects in Organic Chemistry, Verlag Chemie, New York, 1979.
[12] S. Mason, J. Chem. Soc. 219 (1960) (2071 (1954)).
[13] R. Stewart, N. Davidson, J. Chem. Phys. 39 (1963) 255; Biopolymers Symp. 1 (1964) 465.
[14] E. Rosa, W. Simpson, Personal communication.
[15] D. Voet, W. Gratzer, R. Cox, P. Doty, Biopolymers 1 (1963) 193.
[16] B. Pal, Biochemistry 1 (4) (1962) 558.
[17] L. Clark, I. Tinoco, J. Am. Chem. Soc. 87 (1) (1964) 11.
[18] S. Mason, The Pyrimidines, Interscience Publishers, New York, NY, 1962 (Chapter 13).
[19] Z. Abdullah, PhD Thesis, Queen Mary and Westfield College, University of London, 1989.
[20] H. Borresen, Acta Chem. Scand. 19 (1965) 2100.
[21] S. Mason, J. Chem. Soc. (1959) 1240.
[22] Z. Abdullah, N. Tahir, M. Abas, Z. Aiyub, B. Low, Molecules 9 (2004) 520.
[23] Z. Abdullah, N. Mohd, M. Abas, B. Low, Malaysian J. Anal. Sci. 4 (1) (1996) 417.
[24] Z. Abdullah, Bul. Kimia 5 (2) (1990) 72.
[25] Z. Abdullah, N. Waldron, Malaysian J. Chem. 6 (1) (2004) 114.
[26] M. Masoud, S. Haggag, H. El-Nahas, N. Abd-El-Hi, Acta Chim. Hung. 130 (6) (1993) 783.
[27] L. Vares, A. Koulov, B. Smith, J. Org. Chem. 68 (26) (2003) 10073.
[28] D. Brown, A. Todd, S. Varadarajan, J. Chem. Soc. (1956) 2384.
[29] K. Bouhadir, J. Zhou, P. Shevlin, Synth. Commun. 35 (2005) 1003.
[30] O. Mitsunobu, Synthesis (1981) 1.
[31] T. Jenny, S. Benner, Tetrahedron Lett. 33 (1992) 6619.
[32] T. Jenny, N. Previsani, S. Benner, Tetrahedron Lett. 32 (1991) 7029.
[33] J. Zhou, P. Shevlin, Tetrahedron Lett. 39 (1998) 8373.
[34] R. Shatila, K. Bouhadir, Tetrahedron Lett. 47 (2006) 1767.
[35] H. Hammud, A. Ghannoum, M. Masoud, Spectrochim. Acta A 63 (2006) 255.
[36] R. Gup, B. Kirkan, Spectrochim. Acta A 64 (2006) 809.
[37] A. Hasanein, M. Masoud, H. Habeeb, Spectrosc. Lett. 21 (6) (1988) 481.
[38] M. Masoud, S. Haggag, H. El-NAhas, N. Abd El-Hi, Acta Chim. Hung. 130 (6) (1993) 783.
[39] N. Valentic, G. Uscumlic, M. Radojkovic, J. Serb. Chem. Soc. 65 (2) (2000) 81.
[40] G. Wenska, M. Insinska, B. Skalski, Polish J. Chem. 74 (2000) 659.
[41] N. Rajendiran, M. Swaminathan, Ind. J. Chem. 40A (2001) 331; J. Photochem. Photobiol. A Chem. 93 (1996) 103; N. Rajendiran, M. Swaminathan, Bull. Chem. Soc. Jpn. 69 (1996) 2447; N. Rajendiran, M. Swaminathan, Int. J. Chem. Kinet. 29 (1997) 861.
[42] H. Dogra et al., Can. J. Chem. 69 (1991) 1539; S. Dogra et al., Chem. Phys. 226 (1998) 285.
[43] Y. Tsuchiya, T. Tamura, M. Fuji, M. Ito, J. Phys. Chem. 92 (1998) 1760.
[44] M. Daniels, W. Hauswirth, Science 3972 (1971) 675.
[45] S. Undenfriend, P. Zaltzman, Anal. Biochem. 3 (1962) 49.
[46] T. Gustavsson, N. Sarkar, E. Lazzarotto, D. Markovitsi, R. Improta, Chem. Phys. Lett. 429 (2006) 551.
[47] E. Lippert, Z. Natureforsch. 10a (1955) 541; Z. Electrochem. 61 (1957) 962.
[48] N. Mataga, Y. Kaifu, M. Koizumi, Bull. Chem. Soc. Jpn. 28 (1955) 690; Bull. Chem. Soc. Jpn. 29 (1956) 465.
[49] C. Parker, Photoluminescence of Solutions, Elsevier, Amsterdam, 1968.